SUPPORTING INFORMATION

for

Coronene diimide-based '*bowl*' nanostructures as Red Emitter for analysis of Latent fingerprints and metal ion detection

Prabhpreet Singh*[a] and Poonam Sharma[b]

[a]*Department of Chemistry, UGC Centre for Advanced Studies, Guru Nanak Dev University, Amritsar 143 005, India.Tel: +91-84271-01534*

Email: prabhpreet.chem@gndu.ac.in

TABLE OF CONTENTS

1. Experimental section

Materials and reagents

All the chemicals were purchased from sigma aldrich under HPLC grade. Milli-Q water was used during analysis. Non-porous materials to deposit fingerprints, such as aluminum foil, glass slides, metal surfaces etc. were purchased from nearby market.

Instrumentation

1-D (^{1}H and ^{13}C) and 2-D (COSEY) spectra were recorded at 500/125 MHz using Bruker Ascend 500 spectrometer using $CDCl_3$ as solvents. Fourier transform infrared (FT-IR) spectrum of synthesized material was recorded on Cary 630 FTIR spectrometer (Agilent Technologies). Absorption and Emission spectra were recorded on Shimadzu-1900 spectrophotometer and Shimadzu-RF 6000 spectrofluorometers (Shimadzu, Japan), respectively, using quartz cuvettes with a slit width of 5 nm at room temperature. Atomic force microscope (AFM) to image 3-D textures of surface were recorded on Tosca 400 instrument developed by Anton Paar. DLS data was recorded at 25.0 ± 0.1°C using a light scattering apparatus, Zetasizer, Nano-ZS, Nano Series, Malvern Instruments (Malvern, U.K.). Photographs of the developed fingerprints were taken under a UV lamp (365 nm).

Electrochemical Studies

Metrohm Autolab PGSTAT302N electrochemical workstation was employed for recording cyclic voltammetry (CV) at room temperature. Three-electrode cell system containing a Pt working electrode, Pt wire as counter electrode and Ag/Ag^+ (0.1 M $AgNO_3$ in CH_3CN) as reference electrode have been used. Cyclic voltammogram (CV) was recoded at a scan rate of 50 mVs^{-1} in the potential range of −1.6 to 2.0 V vs Ag/Ag^+. The DCM was used as organic solvent and 0.1 M tetrabutylammonium perchlorate (TBAP) as supporting electrolyte for the voltammetry measurement. The NOVA software was used to collect, plot and analyze the raw data of electrochemical measurements of **CDI 2** compound. The HOMO and LUMO energy levels of **CDI 2** were calculated from the cyclic voltammogram of **CDI 2** by using the equation $E_{LUMO} = -[E_{red}(onset) + 4.4]$ eV and $E_{HOMO} = -[E_{ox}(onset) + 4.4]$ eV.

Thermal Gravity Analysis (TGA)

The thermogravimetric analysis (TGA) of **CDI 2** was carried out on HITACHI thermogravimetric analyzer (Model STA7200) under N_2 atmosphere. The non-isothermal decomposition was recorded at a fixed heating rate of 10 ℃/min ranging from 25 ℃ to 1000 ℃. A platinum crucible was used to hold sample in pan. Initially 4.45 mg sample was taken to run the experiment.

UV-Visible and Fluorescence Studies

Stock solutions for various measurements of **CDI 2** were prepared in DMSO and dilutions of these stock solutions were used for the photo physical measurements. The solutions were diluted with DMSO and water before taking the readings in quartz cells. All absorption and fluorescence scans were processed in Excel™ to produce all graphs shown.

Sample preparation for DLS and AFM measurements

The stock solutions of **CDI 2** (1 mM, DMSO) and water were filtered through Millipore membrane filter (Acrodisc syringe filter, 0.2 μm Supor membrane) before measurements to remove suspended impurities. Solutions (10 μM concentration) of **CDI 2** in DMSO and H_2O-DMSO (1:1 v/v; 9:1 v/v) were prepared. 2 mL of each of these solutions was taken in glass cuvette to record the DLS spectrum. Samples for AFM analysis were prepared by drop cast method (~5 μL of aliquot of prepared sample) on glass slides.

Colour purity index

Colour purity of **CDI 2** was also calculated using the Colour Calculator software from Osram Sylvania Incorporated according to equations defined by the CIE (International Commission on Illumination).

Method for Latent fingerprint development

Volunteers were chosen to collect fingerprints on various substrates. Before the collection of fingerprints on various substrates, the donors were asked to wash their hands thoroughly with handwash and dry them properly in air to remove the oily dust. Then fingerprints were collected by softly rubbing the finertip across forehead and then deposited on the substrates with minimum pressure. Then these LFPs were developed with **CDI 2** using powder-dusting method. These developed fingerprints were visualized under 365 nm illumination and captured using the mobile phone camera. The powder-dusting procedure in our system is advantageous over previous systems because no additive or cyanoacrylate fuming, professional training and heavy instrumentation required to image LFPs on non-porous substrates.

*Synthetic Strategy of **CDI 2***

The **PDI I** (50 mg, 0.079 mmol) was dissolved in 5-7 mL CH_3CN in a round bottom flask and then irradiated by sunlight for 7-8 h with continuous stirring. Consumption of the starting material during the reaction was monitored through TLC in $CHCl_3$. Upon consumption of the starting material (TLC), the solvent was removed by using rotatory evaporator to get reddish-orange colored crude product. Further purification was performed by chromatography on silica gel (SiO_2) in Chloroform: Hexane 9:1 to yield orange coloured product (48.2 mg, 96.2%).

^{1}H NMR (500 MHz, $CDCl_3$, 25 °C): δ 10.02 (s, 1H), 9.22 (s, 1H), 9.17 (m, 3H), 9.02 (d, J = 8.1 Hz, 1H), 8.56 (s, 1H), 8.41 (d, J = 7.8 Hz, 1H), 5.28 – 5.17 (m, 2H), 5.02 (d, J = 2.3 Hz, 2H), 2.66 (t, J = 2.3 Hz, 1H), 2.49 – 2.36 (m, 4H), 2.16 – 2.03 (m, 4H), 1.06 (m, 12H) (Figure S1a-b).

^{13}C NMR (125 MHz, $CDCl_3$, 25 °C): δ 150.06, 134.30, 133.44, 132.84, 130.28, 129.49, 128.78, 128.65, 127.35, 126.83, 125.18, 124.80, 124.61, 124.51, 124.05, 79.19, 75.54, 62.46, 59.57, 29.83, 25.24, 11.45 (Figure S1c).

FT- IR spectrum (ATR): ν_{max} [cm^{-1}] = 2929.7, 2877.5, 2340.8, 2117.1, 1915.9, 1699.6, 1654.9, 1595.3, 1423.8, 1312.0, 1252.4, 1155.5, 1043.7, 1006.3, 931.8, 805.1, 745.4 (Figure S1e).

UV/Vis ($CHCl_3$): λ_{max} (ε) = 473 nm (20300), 508 nm (30600) (Figure S3).

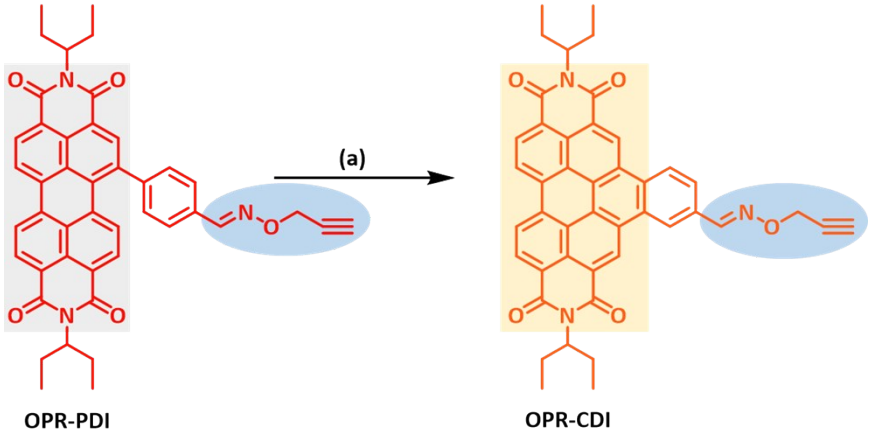

Scheme S1: Synthetic scheme to prepare **CDI 2** through photocyclization of **PDI 1** in CH_3CN, 7-8 h.

2. Characterization data of CDI 2

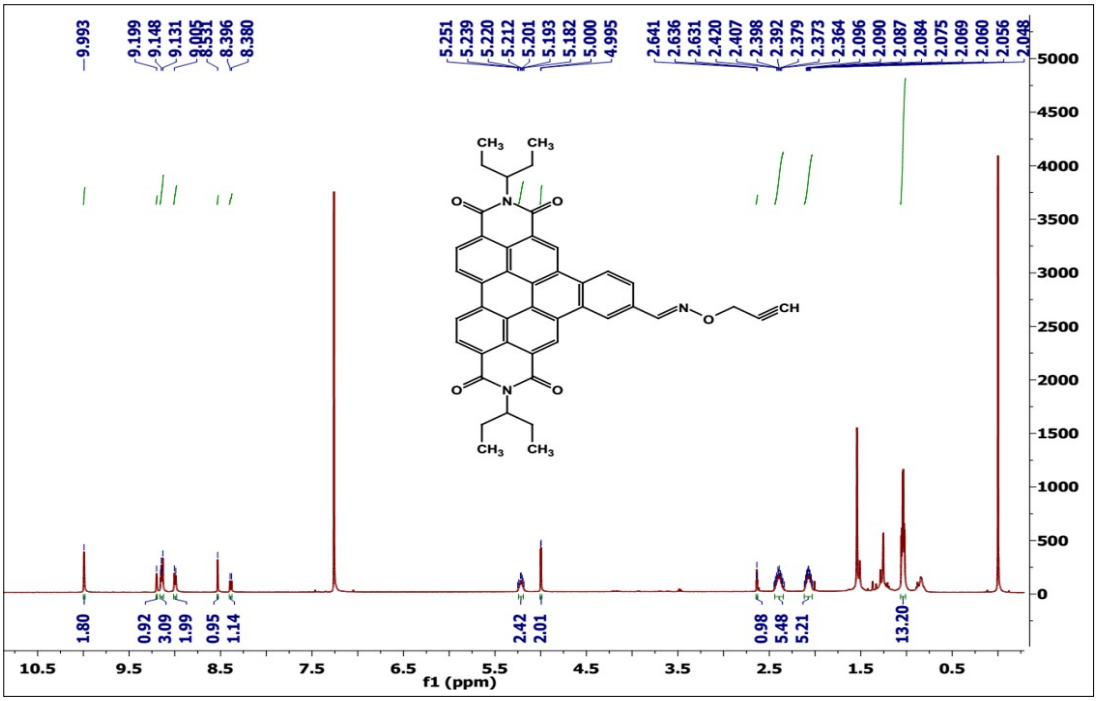

Figure S1a: ^{1}H NMR spectrum of **CDI 2** in $CDCl_3$.

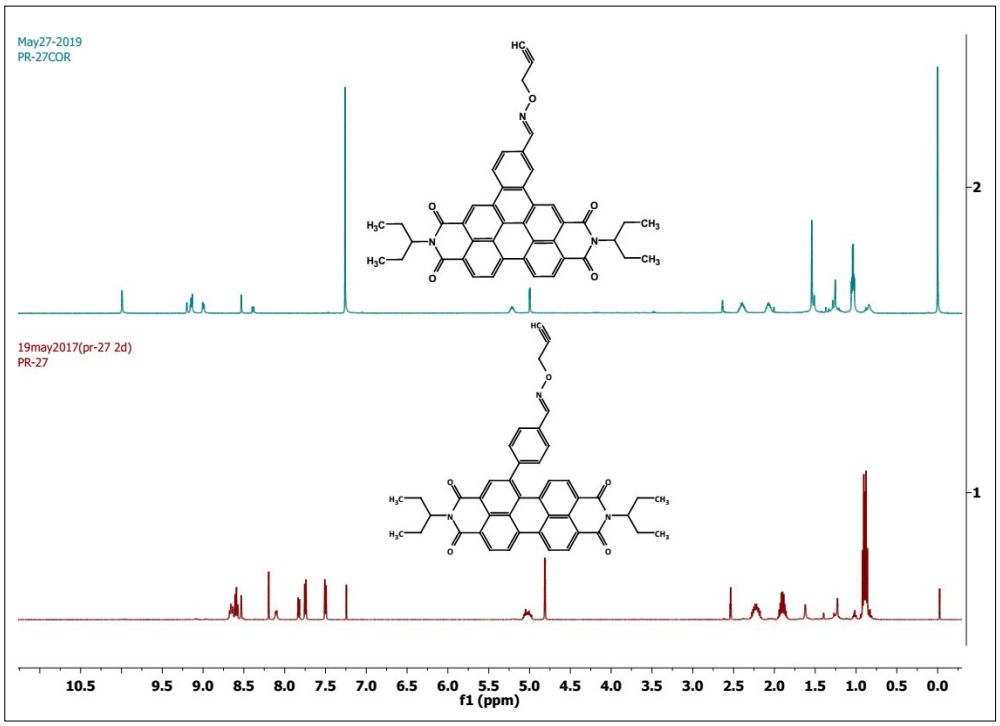

Figure S1b: Comparison of ^{1}H NMR spectrum of **OPR-PDI** and **CDI 2** in $CDCl_3$.

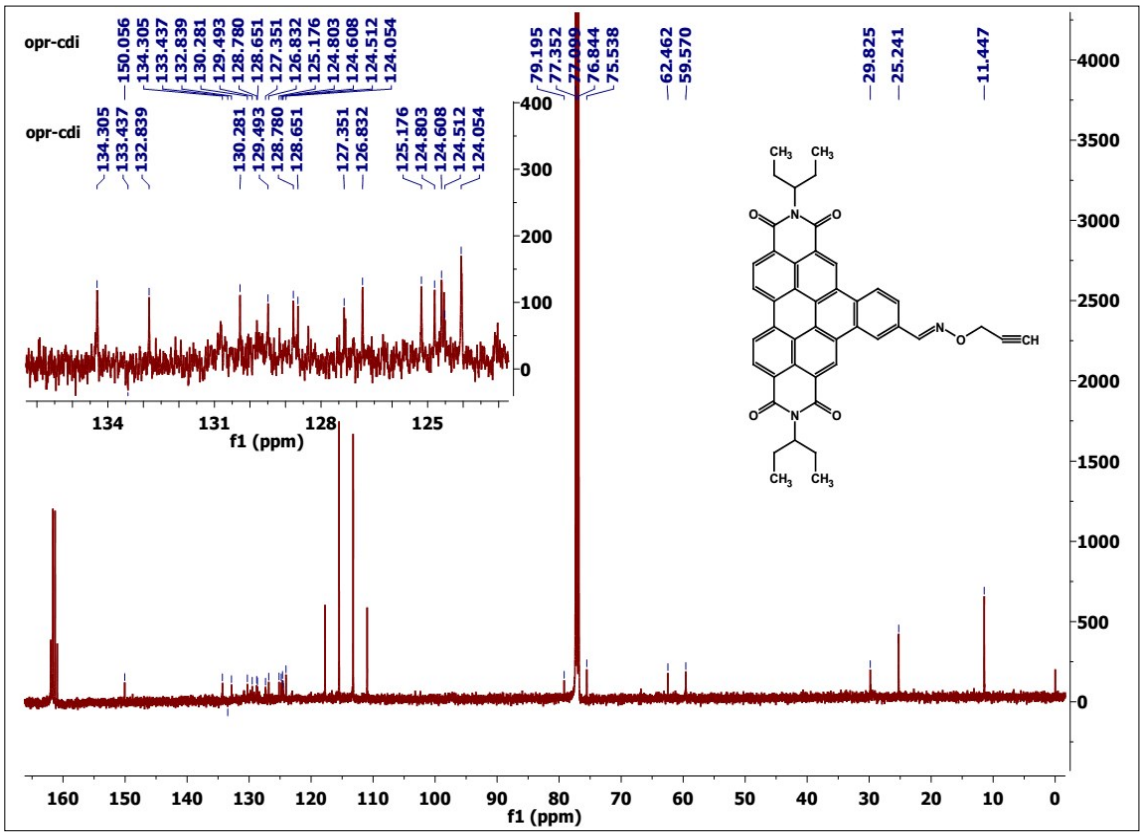

Figure S1c: ^{13}C NMR spectrum of **CDI 2** with one drop of TFA in $CDCl_3$.

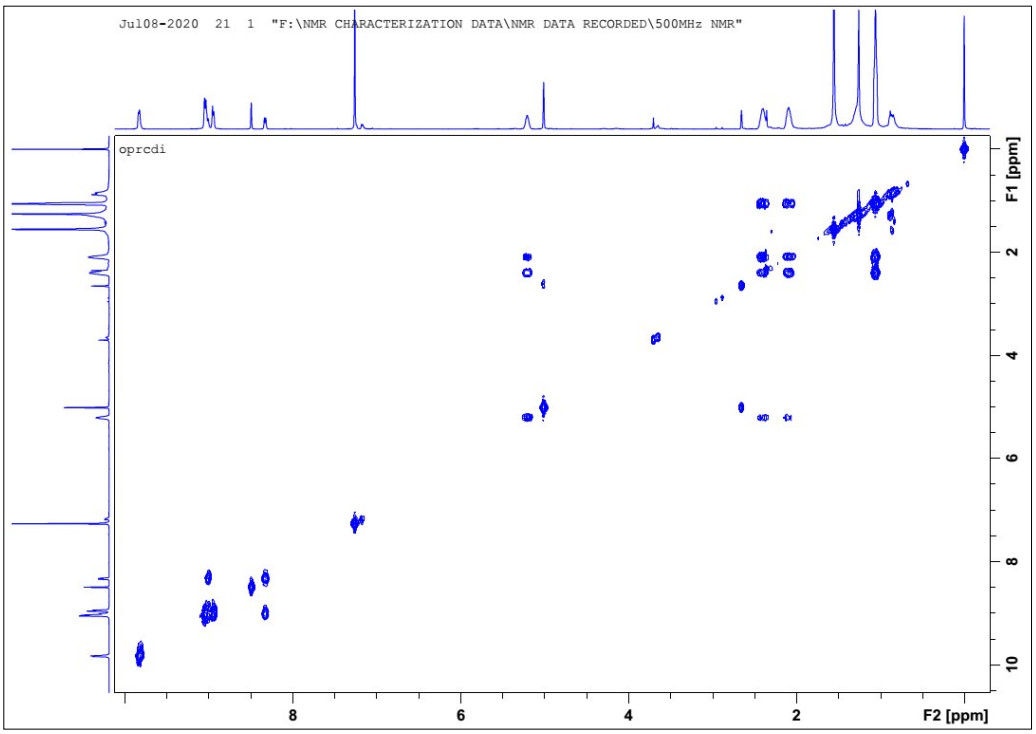

Figure S1d: ^{1}H-^{1}H Correlation (COSEY) spectrum of **CDI 2** in $CDCl_3$.

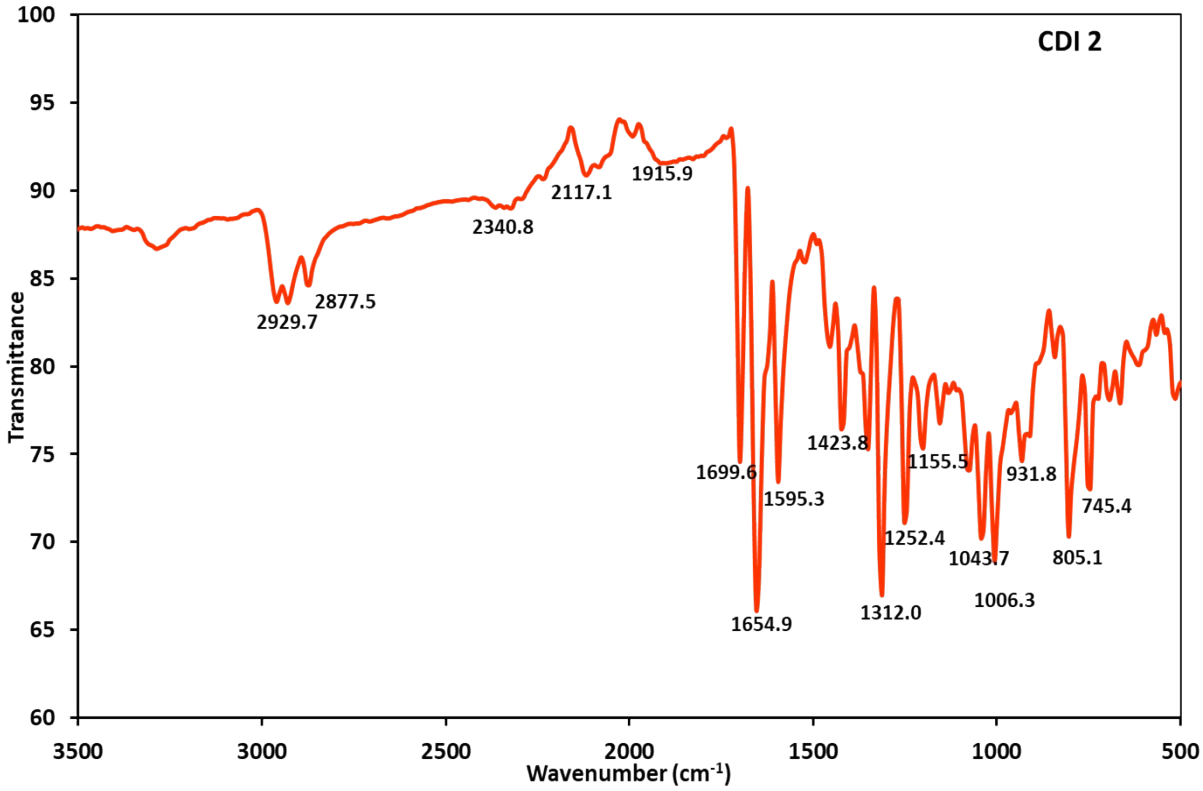

Figure S1e: FTIR spectrum of **CDI 2**.

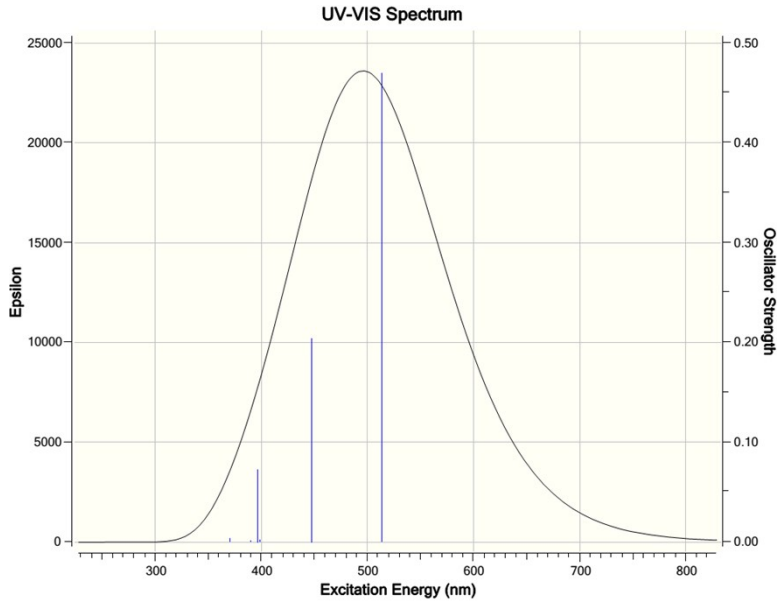

Figure S2: UV-Vis spectrum of **CDI 2** calculated in gas phase using time dependent-density functional theory (TD-DFT) calculations at the B3LYP/6-31G basis Set.

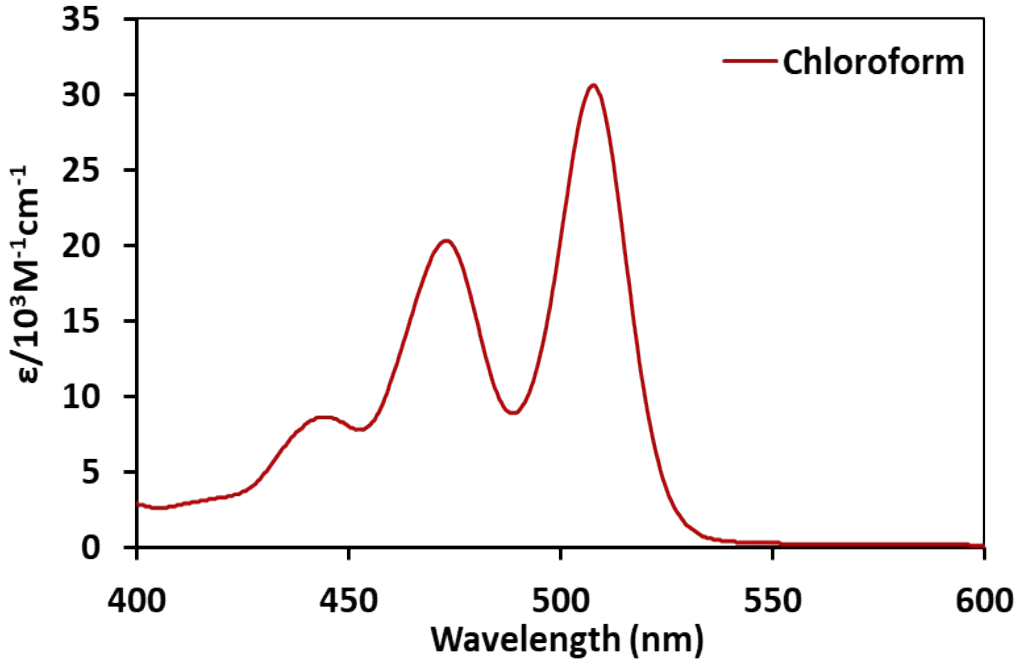

Figure S3: Absorption spectrum (10 μM) of **CDI 2** in chloroform.

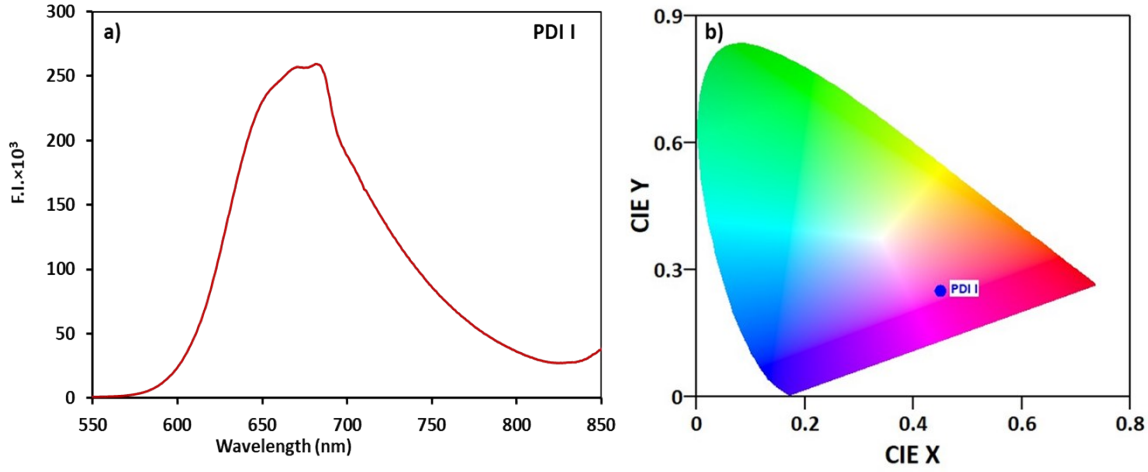

Figure S4: (a) Emission spectrum of solid **PDI 1** and (b) CIE-1931 plots corresponding to emission data of **PDI 1.**

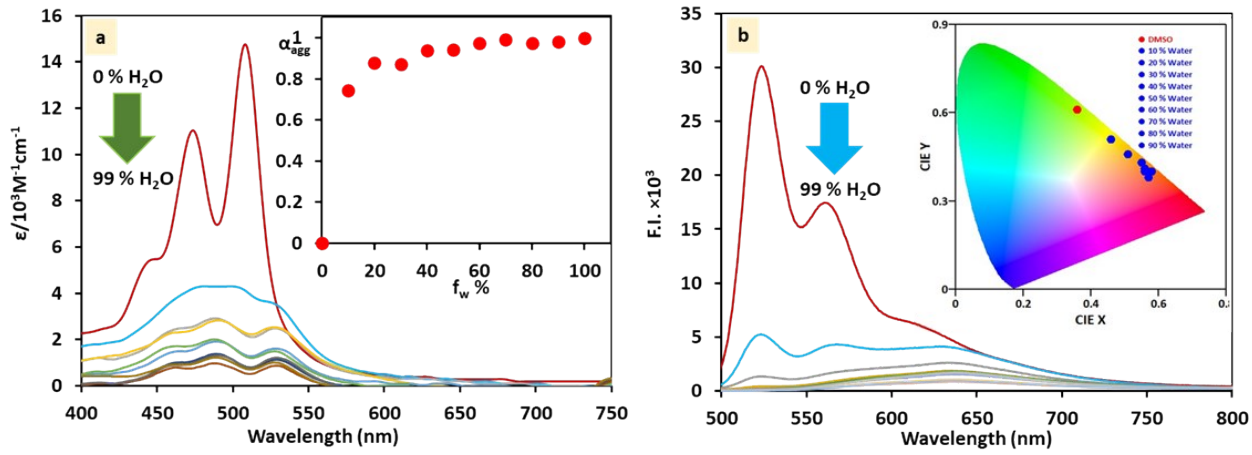

Figure S5: a) Absorption and b) emission spectra of **CDI 2** (10 μM) in different ratios of H_2O and DMSO.

Table S1: Franck-Condon factor ($A_{0\text{-}0}/A_{0\text{-}1}$) values for **CDI 2** in 0–90% H_2O-DMSO binary mixtures.

	508 nm	***474 nm***	
Water Ratio(%)	**$A_{0\text{-}0}$**	**$A_{0\text{-}1}$**	**$A_{0\text{-}0}/A_{0\text{-}1}$**
0	14757.82	11035.17	1.337344
10	4129.154	4222.331	0.977932
20	2195.851	2562.092	0.857054
30	2277.543	2412.461	0.944075
40	1344.093	1581.734	0.849759
50	1269.084	1742.703	0.728227
60	832.5588	1064.837	0.781865
70	545.8687	771.3584	0.707672
80	838.0484	997.5219	0.84013
90	728.8522	936.3005	0.778438

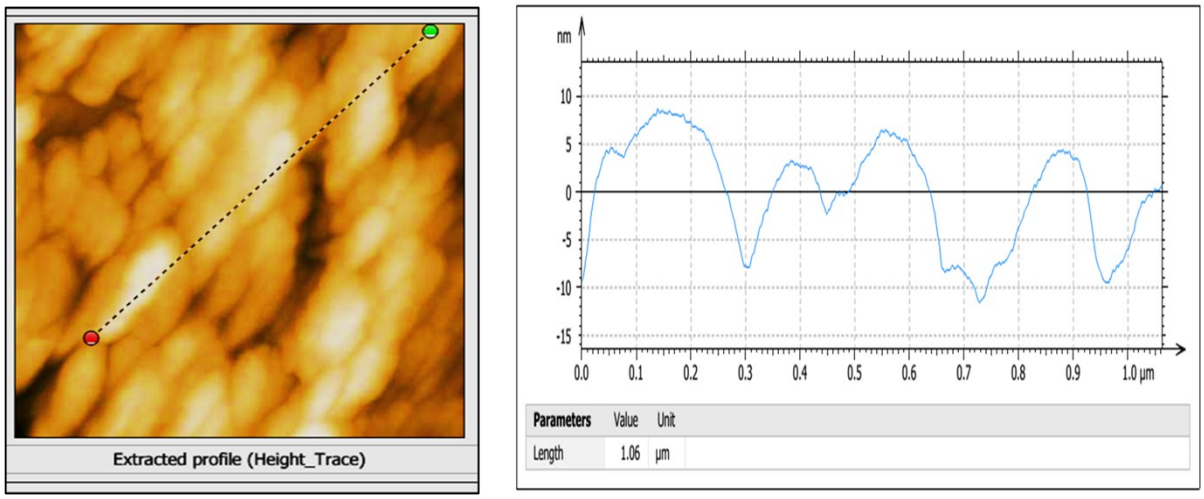

Figure S6a: Height trace extracted profile of AFM micrograph of **CDI 2** in DMSO showing ovaloid morphology with diameter graph.

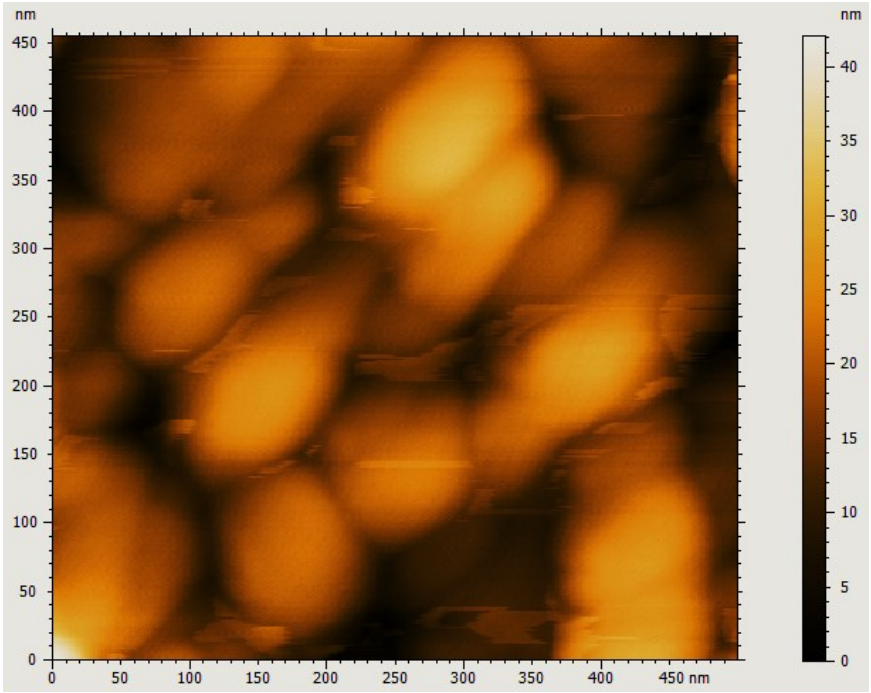

Figure S6b: AFM micrograph of **CDI 2** in 50% H_2O-DMSO binary mixture clearly showing oval and spherical morphology

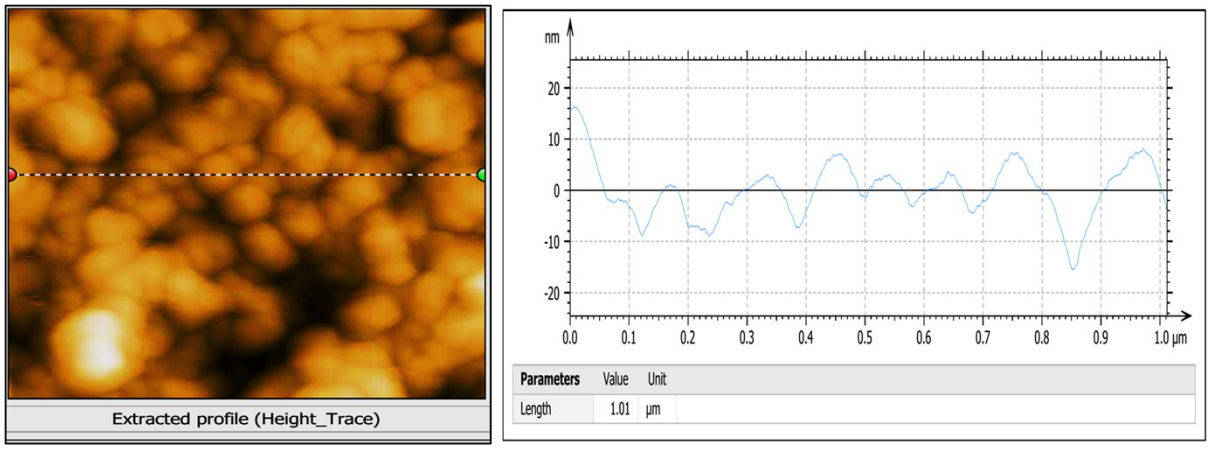

Figure S6c: Height trace extracted profile of AFM micrographs of **CDI 2** in 50% H_2O-DMSO binary mixture showing spherical morphology with diameter graph.

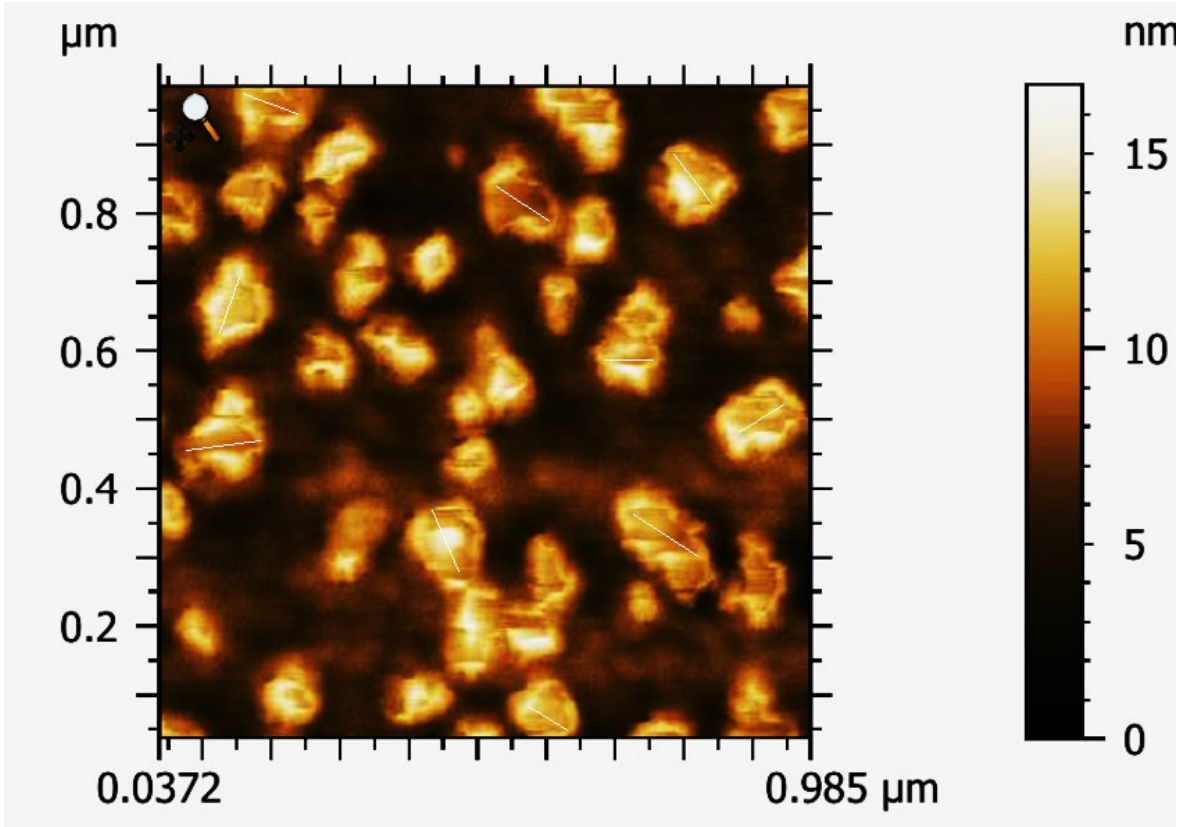

Figure S6d: AFM micrograph of **CDI 2** in 90% H_2O-DMSO binary mixture showing diameter of hollow cavity in the centre of interlinked fibroid morphology calculated by imagej software.

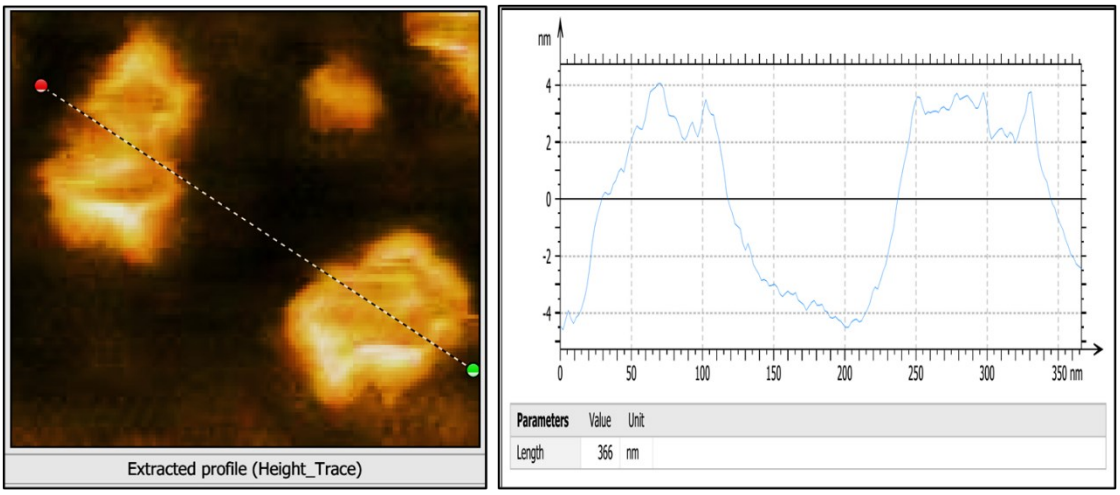

Figure S6e: Height trace extracted profile of AFM micrograph of **CDI 2** in 90% H_2O-DMSO binary mixture showing interlinked fibroid morphology with diameter graph and depth of the cavity.

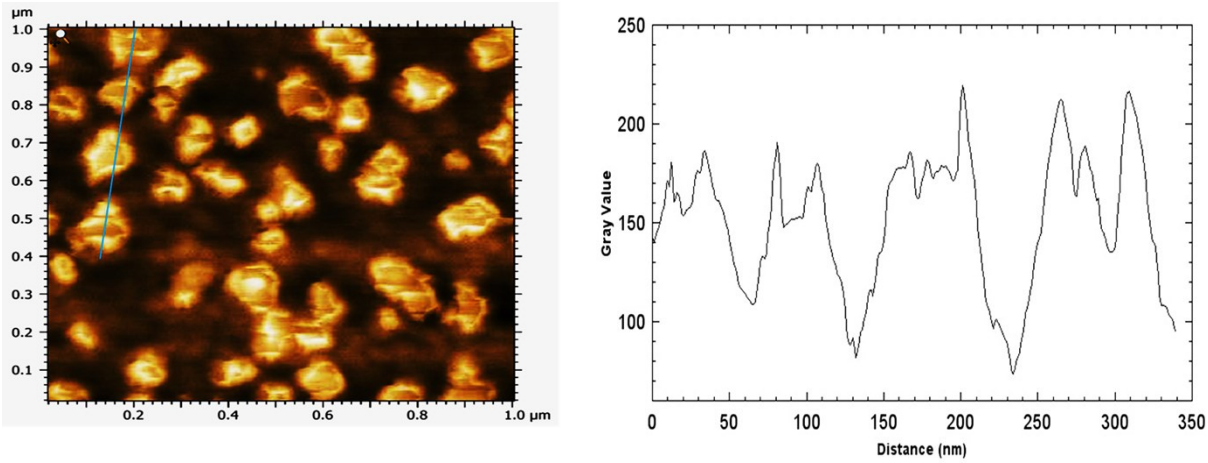

Figure S6f: Variation of the gray value of AFM micrograph of **CDI 2** in 90% H_2O-DMSO binary mixture also showing inner hollow cavity.

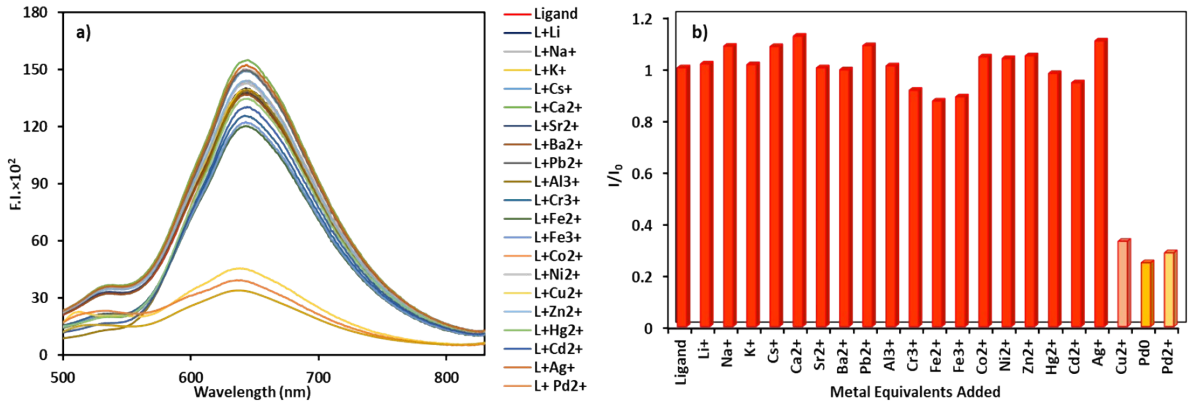

Figure S7: Emission spectra of **CDI 2** (5 μM) in the presence of different metal analytes recorded in 90% HEPES buffer : DMSO (10^{-2} M, pH 7.2) solution; slit width (Ex/Em) = 15/10 nm. Plot of (b) I/Io(emission) versus metal equivalents added.

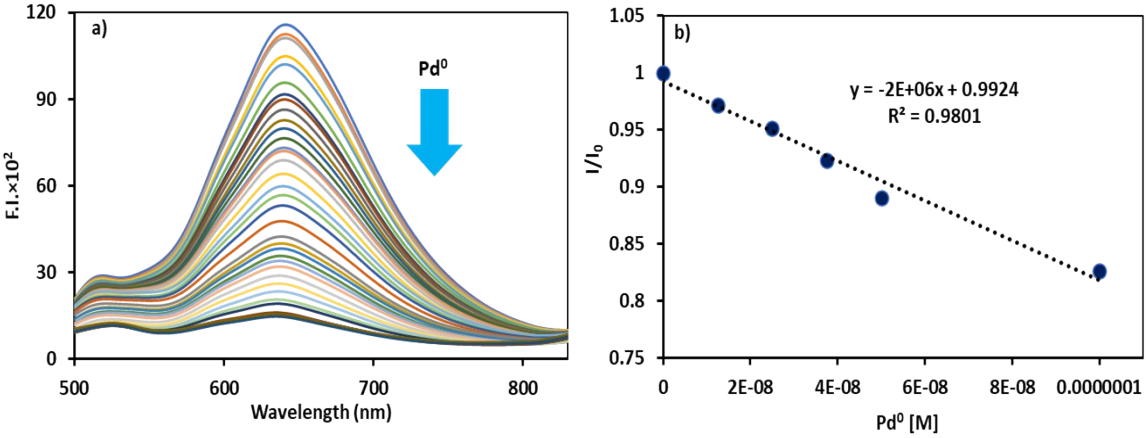

Figure S8: Emission spectra of **CDI 2** (5 μM) in the presence of Cu^{2+} ions recorded in 90% HEPES buffer : DMSO (10^{-2} M, pH 7.2) solution; slit width (Ex/Em) = 15/10 nm. Plot of (b) I/Io(emission) versus concentrations of Pd^{0} ions to determine the lowest detection limits.

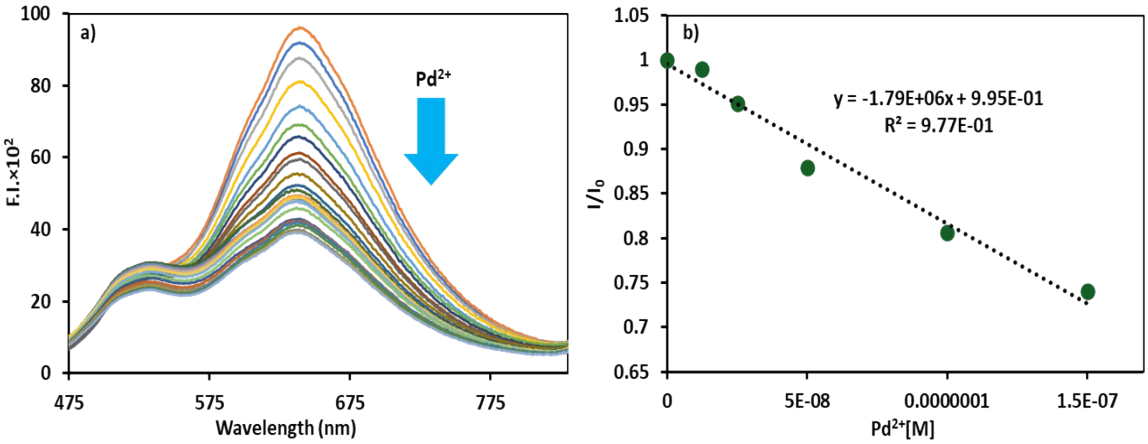

Figure S9: Emission spectra of **CDI 2** (5 μM) in the presence of Cu^{2+} ions recorded in 90% HEPES buffer : DMSO (10^{-2} M, pH 7.2) solution; slit width (Ex/Em) = 15/10 nm. Plot of (b) I/Io(emission) versus concentrations of Pd^{2+} ions to determine the lowest detection limits.

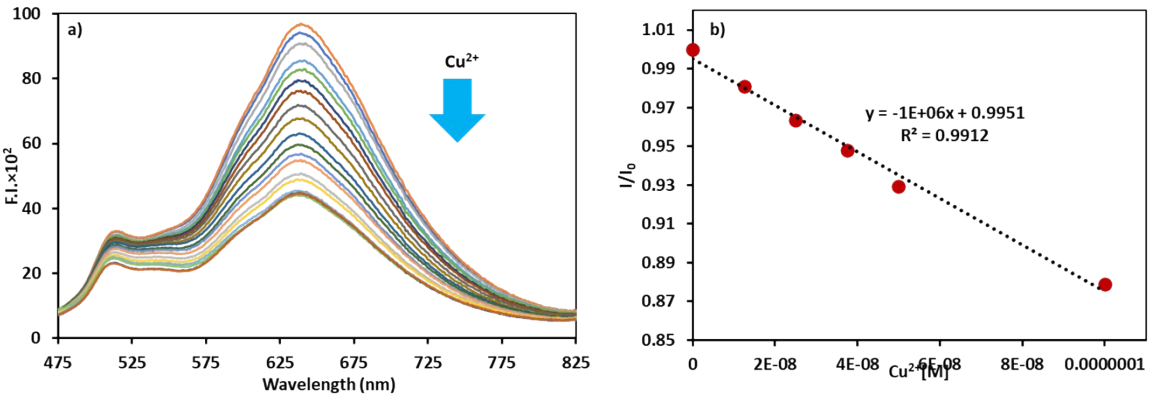

Figure S10: Emission spectra of **CDI 2** (5 µM) in the presence of Cu^{2+} ions recorded in 90% HEPES buffer : DMSO (10^{-2} M, pH 7.2) solution; slit width (Ex/Em) = 15/10 nm. Plot of (b) I/Io(emission) versus concentrations of Cu^{2+} ions to determine the lowest detection limits.

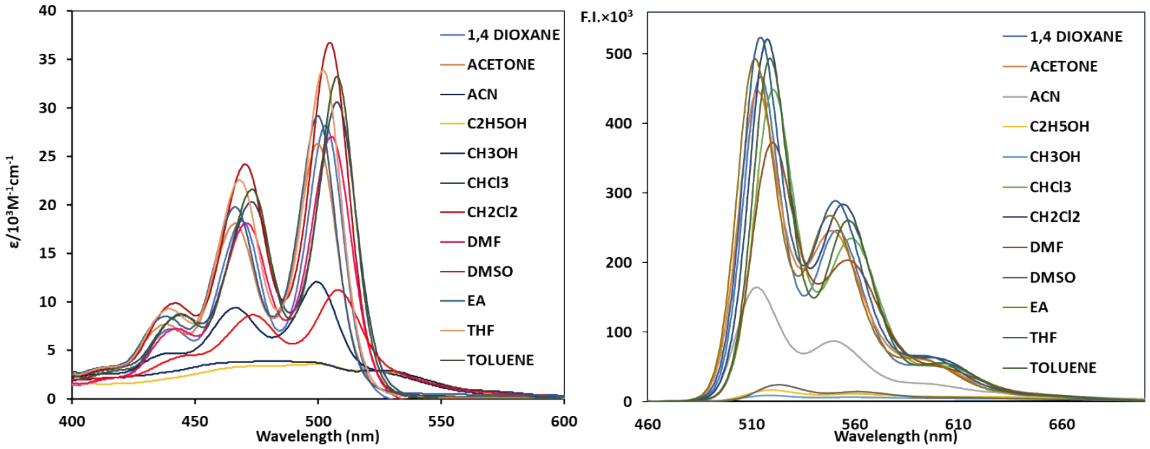

Figure S11: Absorption and emission spectra of **CDI 2** (10 µM) in different solvents.

Table S2: Comparison of some previously reported fluorescent materials for LFP development

Ref.	Type of quantification	Additives Added/Pre or Post Treatment	Method to develop	Type of Surface Used	Visual Assesment	Emission Intensity	Development Time	Features Extracted
1.	Fluorescent Nanomaterials	polyvinylpyrrolidone PVP coating	powder dusting method	porous and nonporous	under illumination method	Not mentioned	4 min. 30 s excitation at 455 and 525 nm	Level 3
2.	NIR fluorescent polymer	ninhydrin	Solid spray	porous and	Also visible to naked eyes	Not mentioned	-	Level 3

				nonporous				
3.	NIR-to-NIR upconversion nanoparticles of β-NaYF4:2% Tm, 48%Yb	-	powder dusting method	-	under illumination method	Not mentioned	0.5−1 h	Level 2
4.	Al(III) Schiff Base	Au^{3+}	powder dusting method	smooth surfaces	under illumination method	418- 572 nm	-	Not mentioned
5.	Fluorescent dyes	-	0.1g/100mL dye solution	sticky side of adhesive tapes	under illumination method	447-499 nm	0.5–2 min.	Not explained
6.	Fluorescent dyes	pretreatment with (0.01 M, pH 12.0) NaOH Sol.	2.0×10^{-4} M dye in ethanol: aqueous sodium hydroxide (1:1,v/v)	porous	naked eye and under illumination method	Not mentioned	1 h and 40 min.	Not explained
7.	Fluorescent Metal Complexes emitting deep blue light	Zn^{2+} metal added	powder dusting method	nonporous	under illumination method (366 nm)	Not mentioned	-	Not explained
8.	AIE active Fluorescent dyes	-	70% H_2O:THFmixture (0.3 mM)	non-porous	under UV 365 nm light	Not mentioned	3 min.	Level 2
9.	Dual state emission platform	traditional magnetic powders	powder dusting method	-	nonporous	under illumination method	Not mentioned	Level 2
10.	Fluorescent nanomaterial	-	50% H_2O:CH_3CN mixture	nonporous	under illumination method	Not mentioned	-	Level 2
11.	Fluorescent dyes	pretreatment of bloody stains with ethanol: water (40:60) in 2% 5-sulfosalicylic	0.1g/100mL dye solution	porous, semi-porous and non-porous	bloody fingermark	Not mentioned	-	Not explained

		acid						
12.	AIE-active luminogen	cyanoacrylate fuming	CH_3CN –water solution aggregates	nonporous	under illumination method	Not mentioned	20 minutes	Level 3

Table S3: Comparison of some previously reported fluorescent materials based on benzocoronene.

S. No.	Synthetic Mechanism of CDI	Self-assemblies Properties	Energy and electron transfer properties	Applications
1.	Photo-cyclization	Not mentioned	Visible-light triggered photo-annulation approach	Photo-responsive materials
2.	Imidization with 2,6-diisopropylaniline	Not mentioned	Non-fullerene acceptors and tuneable optical and redox properties	Optoelectronic materials
3.	Not mentioned	Not mentioned	Electron acceptors	To study ultrafast photoinduced intramolecular electron transfer
4.	Not mentioned	Surface morphology Studied with AFM	4-octyltetradecyl side chains exhibits the highest electron mobility of 0.16 $cm^2V^{-1}s^{-1}$	n-type organic semiconductors
5.	Cyclodehydrogenation with DDQ in dry CH_2Cl_2 at 0^oC	Showing thermotropic liquid crystalline behavior		Used as a “turn-on” probe for Pb2+or K+
6.	Benzogenic Diels–Alder reaction	Self-assembled nanofibers in aqueous solution	Not mentioned	Showing peroxidase-like catalytic activity for H2O2and glucose sensing
7.	Sunlight-driven photocyclization inCH_2Cl_2	Self-assembled (fibre-to-disc)	Not mentioned	Biolabeling and visualization of latent fingerprints on

		fluorescent aggregates		different surfaces
8.	Sunlight-driven photocyclization	Aggregation in 30 % DMF: H2O	Not mentioned	Imaging of latent fingerprints on non-porous and porous substrates
Present Manuscript	Photocyclization in CH_3CN	Nano-sized interlinked fibre structures forming '*bowl*' shaped nanoarchitecture	Red emitters with CIE coordinates (x,y) of (0.67, 0.33) with 100 % colour purity	For visualization of latent fingerprints (LFPs) and metal ion detection in aqueous medium